DUVAR KİTABEVİ
ISBN: 978-625-7502-79-5

insac

NATURAL AND ENGINEERING SCIENCES

Yazarlar
Chapter 1: Ahmet Demiralp,
Chapter 2: Tayfun Abut,
Chapter 3: Ayşe Elif Ateş,
Chapter 4: Ayşe Elif Ateş,
Chapter 5: Naki Akçar, E. Vural Yavuz,
Chapter 6: Barış Kınacı, Çağlar Çetinkaya, Erman Çokduygulular,
Chapter 7: Hilal Surat,
Chapter 8: İkbal Demet Nane,
Chapter 9: Barış Kantoğlu, Serenay Satılmış,
Chapter 10: Erhan Şener,
Chapter 11: Erhan Şener,
Chapter 12: Adile Akpınar,
Chapter 13: Gökhan Kızılışıkoğlu, Ayfer Alper,
Chapter 14: Hatice Banu Keskinkaya, Cengiz Akköz,
Chapter 15: Hülya Sayğı,
Chapter 16: Tufan Gürkan Yılmaz, Fatih Karpat,
Chapter 17: Mehmet Bektaş,
Chapter 18: Ozgur Baser, Ergin Kilic,
Chapter 19: Sabire Yerlikaya, Seyfullah Keleş,
Chapter 20: Onur Miran Öztekin, Naime Filiz Özdil,
Chapter 21: Fatma Tomul, Yasin Arslan,
Chapter 22: Yasin Arslan, Fatma Tomul,
Chapter 23: Büşra Kavasoğlu, Hülya Şen Arslan, Cemalettin Sarıçoban,
Chapter 24: Ahmet Yönetken, Ayhan Erol,
Chapter 25: Gülin Gençoğlu Korkmaz, Yasemin Gündoğdu, Hamdi Şükür Kılıç, Hüseyin Kurt, Recai Kuş,
Chapter 26: Esen Hanaç,
Chapter 27: Hilal Surat,
Chapter 28: Ferda Karakuş

Editör
Doç. Dr. Gizem Mısır
Dr. Mehmet Uzun

INSAC Natural and Engineering Sciences

Editörler
Doç. Dr. Gizem Mısır
Dr. Mehmet Uzun

INSAC

Natural and Engineering Sciences

Doç. Dr. Gizem Mısır
Dr. Mehmet Uzun

Genel Yayın Yönetmeni: Berkan Balpetek
Kapak ve Sayfa Tasarımı: Duvar Design
Baskı: Aralık 2021
Yayıncı Sertifika No: 49837
ISBN: 978-625-7502-79-5

853 Sokak No:13 P.10 Kemeraltı-Konak/İzmir
Tel: 0 232 484 88 68

www.duvaryayinlari.com
duvarkitabevi@gmail.com

Baskı ve Cilt: REPRO BİR
Repro Bir Mat Kağ. Rek. Tas. Tic. Ltd. Şti.
İvogsan 1518. Sokak 2/30 Mat-Sit iş Merkezi Ostim
Yenimahalle/Ankara
Sertifika No: 47381

Discrimination of the Volcanic Units Using Calibration-Free Laser Induced Breakdown Spectroscopy (CF–LIBS)

Gülin Gençoğlu Korkmaz[1], Yasemin Gündoğdu[2,5], Hamdi Şükür Kılıç[3,4,5], Hüseyin Kurt[1], Recai Kuş[6]

[1] Konya Technical University, Faculty of Engineering, Department of Geological Engineering, Konya, Turkey
[2] Selcuk University, Kadınhanı Faik İçil Vocational School, Department Of Computer Technologies, Konya, Turkey
[3] Selcuk University, Faculty Of Science, Department Of Physics, Campus, Selçuklu, Konya, Turkey
[4] Selcuk University, Advanced Technology Research And Application Center, Campus, Selçuklu, Konya, Turkey
[5]Selcuk University, Laser Stimulated Proton Therapy Application And Research Center, Campus, Selçuklu, Konya, Turkey
[6] Selcuk University, Faculty Of Tecnology, Department Of Mechanical Engineering, Campus, Selçuklu, Konya, Turkey

1. Introduction

The understanding and exploring of the rocks are significant as they have critical signals concerning how they originated and evolved within the time. Sometimes, they may be used as a tool for detecting hazardous and nuclear chemicals, and explosive traces.(De Lucia & Gottfried, 2011). The rocks could be monomineralic or polymineralic and they are classified into three major groups based on how they formed: igneous (volcanic, sub-volcanic, plutonic rocks), metamorphic and sedimentary rocks. However, enclave term is used for crystal clots (clusters) in the rocks and differ from the host rock in which it is located, disrupting the homogeneous appearance of the host-rock (Bernard Barbarin & Didier, 1992). Enclaves may be distinguished from the host-rock in terms of color, shape, size, texture, and mineralogical composition macroscopically and/or microscopically. Based on formation, origines, and relationships with felsic host rocks, the enclaves have been classified as (1)Xenolite, (2) Restite, (3) Cognate enclave (Magma Segregation Enclaves) (4) Microgranular enclave (B Barbarin & Didier, 1991; Best, 2003; Cantagrel, Didier, & Gourgaud, 1984; Dahlquist, 2002; Didier, 1991; G. Gençoğlu Korkmaz, Kurt, & Asan, 2021; Ilbeyli & Pearce, 2005; Kadioglu & Gülec, 1996; Kadıoğlu & Güleç, 1999; Kocak, Zedef, & Kansun, 2011; Kumar, 2010; Kumar, Rino, & Pal, 2004; Kumar & Singh, 2014; Noyes, A.F., & Wones, 1983; Özdamar, Zou, Billor, & Hames, 2020; Winter, 2001; Zhang et al., 2020).

The rock forming minerals such as, olivines, clino-ortho pyroxenes, clino-ortho amphiboles, biotites, feldspars, are crucial for main chemical composition of the rocks. The lattice structure of the minerals hold the elements according to their atomic radius, and so they reflects the chemical composition of the rocks(Kalam, Rao, Jayananda, & Rao, 2020). For instance, the lattice of the clinopyroxenes could hold Al, Fe, Ca, Mg, Si, Na cations; amphiboles and biotites hold Si, Mg, Al, K, Fe cations; plagioclases have Na, Al, Si and Ca cations; titanites include Ca, Ti, and Si cations into their structure (Gülin Gençoğlu Korkmaz, Gündoğdu, Kılıç, & Kurt, 2021). The structure of olivine allows that its crystal sites offer room for only are stricted number of trace elements. Generally, rare earth elements fit better into the structure of the clinopyroxene and garnet minerals rather than the olivines(Foley, Prelevic, Rehfeldt, & Jacob, 2013).

The chemical characteristic of the rocks could be detected by well-known and conventional methods such as XRF and ICP-MS. Among several analytical methods laser induced breakdown spectroscopy (LIBS) can be potentially utilizied to explore the chemical composition of the rocks. LIBS detects the deverse chemical elements in any sample (generally solid) quantitatively and qualitatively (Miziolek, Palleschi, & Schechter, 2006). LIBS has also been used in several applications such as identification of cancerous cells, tissue classification (Yueh, Zheng, Singh, & Burgess, 2009) for dental and medical studies, classification of plastic polymers (Lasheras, Bello-Gálvez, & Anzano, 2010), archaeological studies (Muhammed Shameem et al., 2020; Remus et al., 2010), space and Martian research (Cousin, Sautter, Fabre, Maurice, & Wiens, 2012) and geological studies (Gondal, Nasr, Ahmed, & Yamani, 2009; Hark & Harmon, 2014; R. Harmon et al., 2009; Russell S. Harmon et al., 2019; Russell S Harmon, Russo, & Hark, 2013; Russell S. Harmon et al., 2018; Kalam et al., 2020; Roux et al., 2015). LIBS is a practical and important method for the determination of the source elemental composition in many fields and studies, since it is advantageous because of the lower cost, remote-sensing capability and the fast results can be obtained from the installed system compared to other chemical analytical techniques such as XRD, XRF, RAMAN, ICP-MS. REEs and some light elements (such as Li, Na) that could not be measured by XRF could be detected with LIBS (Abedin, Haider, Rony, & Khan, 2011; Bhatt, Jain, Goueguel, McIntyre, & Singh, 2018; Lawley, Somers, & Kjarsgaard, 2021), therefore, not only in whole-rock geochemistry studies, but also in natural mineral chemistry and in mineral classification studies such as garnet and carbonate minerals, LIBS is frequently preferred (Gottfried, Harmon, De Lucia, & Miziolek, 2009; R. S. Harmon et al., 2009). The main principle for LIBS technique is that laser pulses are focused onto a sample to execute laser ablation and generation of a laser induced plasma from which the optical emission spectra are received and recorded by a specrometer (Panya panya et

al., 2018). The observed LIBS spectrum reflects the entire elemental composition, i.e. chemical fingerprint, of the sample.

Eventhough nanosecond (ns) laser is predominantly used in LIBS technique, femtosecond (fs) laser is used more appropriately for quantitative principal analysis due to better reproducibility of plasma features (lower relative standard deviation, RSD) (Kalam et al., 2020). Chemical content of any sample could be measured by LIBS with or without any calibration process. If the plasma is in a Local Thermodynamic Equilibrium (LTE) conditions, the calibration-free (CF) LIBS method does not require any calibration process where spectral curves could be utilized in analytical chemistry for calibration (Musazzi & Perini, 2014). The CF-LIBS technique could be utilized on any smooth-surface sample and, can measure accurately any element when the plasma is under the local thermal equilibrium conditions and is optically thin enough(Hamad, Alaa, Salloom, & Ghazai, 2018; Tognoni, Cristoforetti, Legnaioli, & Palleschi, 2009; Umar, Liaqat, Ahmed, & Baig, 2020). Through that favorable side, LIBS has become a popular method, recently. However, the LIBS technique, applied as quantitatively analytical analysis needs to be checked from more well-known and conventional technologies such as the X-Ray fluorescence (XRF), ICP-MS and Raman (Alberghina, Barraco, Brai, Schillaci, & Tranchina, 2011).

Here, we report a case study regarding femtosecond CF-LIBS application on volcanic rocks and their enclaves, and to correlate LIBS and previous XRF (G. Gençoğlu Korkmaz et al., 2021) results. Here, we have calculated the plasma characteristics to validate LIBS data. Also we have operated the principal component analysis (PCA) which is a statistical approach firstly used by Wold, Esbensen, and Geladi (1987) to differentiate the studied rocks and their enclaves by using their LIBS spectra.

2. Experimental Setup

The freshest and most representative four samples (andesitic-dacitic host rocks and their enclaves) from Konya (Central Anatolia) region were selected and analysed in the labratory. Thin sections were made in Ankara University YEBİM for petrographic examination of these rocks, and they were examined under a polarizing microscope in the Geological Engineering Department of Konya Technical University.

The samples, whose altered surfaces were removed, were first powdered in a ball milling in the Selcuk University-Laser Spectroscopy Laboratuary. Then, 0.8 g sample mixed with 0.2 g wax (polyvinyl alcohol). The obtained mixtures were pressed under 50 MPa pressure and 200°C temperature for 30 minutes and turned into pellets, and prepared for the LIBS analysis which the experiemtal set-up is shown in fig.1 in detail.

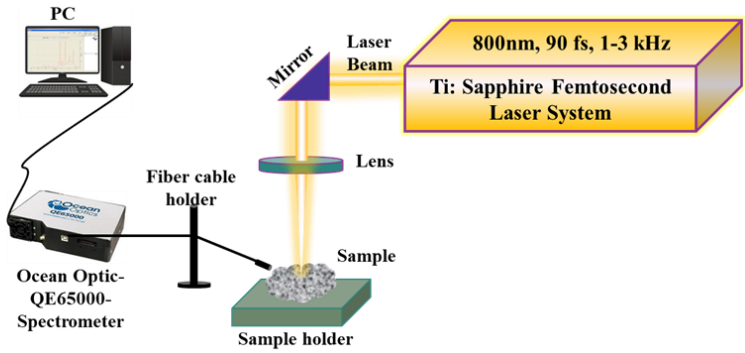

Fig.1 Schematic represation of fs-CF-LIBS experimental set-up

The Ocean Optics, QE65000 spectrometer was used and correlated for this study, and Nd-YAG laser operated at its fundamental wavelength of 800 nm. Laser pulses of 90 fs Ti:Sapphire Femtosecond Laser System at 1800 mJ were focused on the sample. In this study, the analyzes were repeated until the best results were obtained by changing the experimental parameters. First of all, the samples were pressed with and without wax and analyzed. Then, the waxed samples were baked and the wax material was waited for drying and analyzed again. At each stage, laser power was applied on the samples as 500 mW, 1000 mW, 1500 mW, 1800 mW and the analyzes were repeated at several times. According to these data, the conditions in which the most meaningful peaks and optimum results were obtained were determined. It has been observed that the most suitable conditions are provided on waxed-unbaked samples, where high laser power is given.

3. Results and Discussion

3.1. Petrography and Classification of the Rocks

The studied rocks are intermediate lava units and have andesitic-dacitic composition. Also they have hypocrystalline porphyric texture. Pheno and microphenocrysts in the rock are plagioclase, clinopyroxene, amphibole, opaque minerals and rarely biotite and quartz (Fig 2a-b). In the groundmass phase, in addition to these minerals, volcanic glass is also observed in the investigated volcanic rocks (Figs 2 a-b). The investigated andesitic rocks contain magma segregation enclaves (MSE)(G. Gençoğlu Korkmaz et al., 2021). MSE enclaves are in gabbroic rock composition, and contain mainly plagioclase and clinopyroxene phenocrysts and Fe-Ti oxide microphenocrysts. Also, they show a coarse-grained texture as typically in igneous rocks (Figs 2 c-d). Plagioclase grains are zoned and rarely sieved in the hosts. However in the enclaves they are unzoned and dusty sieved (Fig 2). While the pyroxenes in the host rock are euhedral, in the enclaves they are anhedral, fractured and have poorly developed cleavages. In the host rocks,

amphiboles are usually subhedral (Fig 2 a-b), whereas in the enclaves they are anhedral, fractured or bladed/quenched (Figs 2 c-d).

Based on mineralogical, petrographical, chemical properties and geochemical classification diagram TAS (total alkali-silica) (Le Bas, Le Maitre, Streckeisen, & Zanettin, 1986), investigated rocks have been classified as basaltic-andesite, andesite, and dacite (Fig. 3a) (G. Gençoğlu Korkmaz et al., 2021).

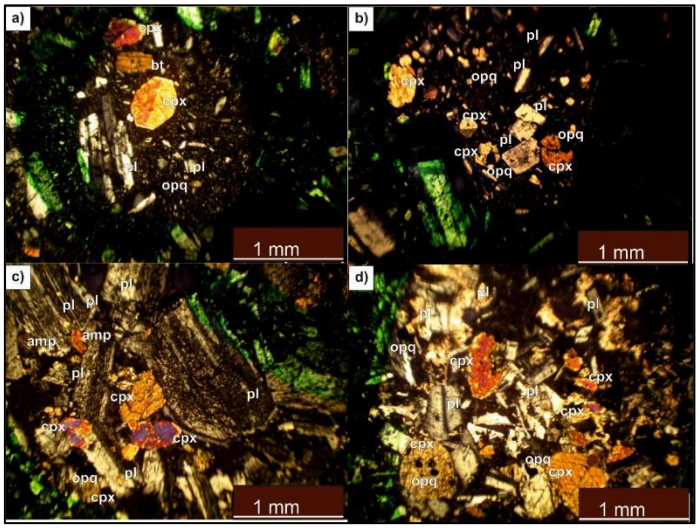

Fig. 2 Photomicrophotographs of the (a) Host rock-1, (b) Host rock-2, (d) enclave-1 (e) enclave-1 (G. Gençoğlu Korkmaz et al., 2021)

Geochemical fingerprinting is a significant term showing the chemical composition of a rock or mineral that reflects the geological processes associated with its evolution. Generally, the trace element composition of the rocks could be used as the major indicators for the evolution and genesis of the rocks. Investigated rocks are high-K calc-alkaline rocks with their K_2O (1-3%wt) contents (Fig 3b). Moreover, enclaves contain lower K_2O and Na_2O and higher MgO, CaO, Al_2O_3 contents relative to their enclaves (Figs 3, 4, and Table 1)(G. Gençoğlu Korkmaz et al., 2021).

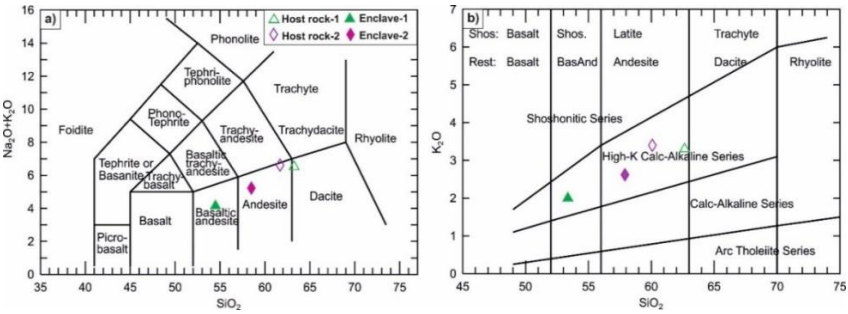

Fig. 3 (a)Total alkali-Silica diagram (Le Bas et al., 1986)and (b) SiO_2 vs.K_2O diagram of the investigated rocks. Data from G. Gençoğlu Korkmaz et al. (2021)

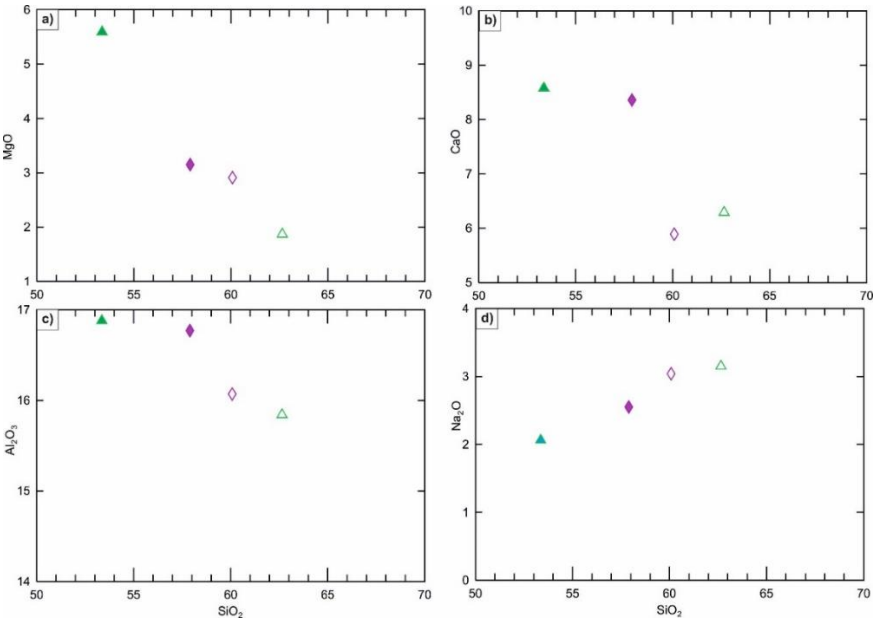

Fig. 4 SiO_2 versus selected major oxide variation diagrams of the investigated rocks. Data from G. Gençoğlu Korkmaz et al. (2021)

The minerals in the rock give information about the elements found in the rock (Table 2). They carry a trace of which elements will be found. For this reason, the identification of the minerals in the rock has a key role in the interpretation of the atomic spectra obtained by the LIBS method. Increasing SiO_2 against decreasing CaO and MgO shows that pyroxenes are fractionated, however, the negative relationship between SiO_2 and Al_2O_3 and the positive relationship between Na_2O and SiO_2 display fractionated plagioclase minerals (Gill, 2010; Rollinson, 1993). These chemical signatures are in agreement with petrographic observations. Moreover, the fact that the enclaves are more primitive with their higher MgO and CaO and lower SiO_2 contents than their hosts suggest that they were formed at an earlier stage

than their hosts and that they are the crystal clots that crystallized in the early stage (G. Gençoğlu Korkmaz et al., 2021) (Table 1).

Table.1 The major oxides (wt%) and some of the trace elements (ppm) of studied rocks acquired from the X-ray fluorescence method (XRF) (G. Gençoğlu Korkmaz et al., 2021).

Sample	Host rock-1	Enclave-1	Host rock-2	Enclave-2	Sample	Host rock-1	Enclave-1	Host rock-2	Enclave-2
Major oxides (%wt.)					Traces (ppm)				
SiO_2	53.36	62.65	58.33	63.58	Ba	510	620.6	496.9	707.7
Al_2O_3	16.88	15.84	14.56	15.16	Ni	58	7.1	22.2	8.4
Fe_2O_3	9.39	5.63	7.59	5.64	Co	46.4	49.4	54.1	56.8
MgO	5.59	1.87	3.84	2.55	Hf	3.9	3	4.2	3.3
CaO	8.58	6.29	9.16	6.55	Nb	12.1	7.8	9.4	12
Na_2O	2.06	3.15	2.57	2.49	Rb	54.7	96.6	70.1	100
K_2O	2	3.3	2.45	2.99	Sr	459.9	532.3	707.2	548.4
TiO_2	0.55	0.56	0.61	0.53	Th	9.3	18.2	13.2	19.1
P_2O_5	0.19	0.21	0.37	0.19	U	18	18.3	20.8	9
MnO	0.22	0.11	0.14	0.11	Zr	141	145.9	105.4	162.3
Cr_2O_3	0.05	0	0.01	0.01	Y	36.7	19.2	19.7	16.7
Sum	98.87	99.61	99.63	99.8	La	47.8	16.5	31.4	28.4
					Ce	81	47.6	62.1	62.9
					Cu	51.7	30.6	69.7	41.1
					Pb	13.4	18.4	20.6	23.7
					Zn	82.3	44.9	56.5	50.9

Table 2 Simplified petrographical and whole-rock geochemical properties of the studied rocks

Sample	Rock type		Composition	Mineral contents	Chemical composition
144	Host Rock-1	Dacite	Intermediate	Plagioclase, biotite, amphibole, clinopyroxene, Fe-Ti oxide, volcanic glass	Dominantly SiO_2, Al_2O_3, K_2O, Na_2O, CaO, more less TiO_2, more less MgO, FeO,
144E	Enclave-1	Gabbro	Mafic	Plagioclase, clinopyroxene, Fe-Ti oxide	Dominantly SiO_2, CaO, MgO, FeO rarely K_2O, Na_2O, TiO_2
161	Host Rock-2	Andesite	Intermediate	Plagioclase, Amphibole, clinopyroxene, Fe-Ti oxide, volcanic glass	Dominantly SiO_2, Al_2O_3, K_2O, Na_2O, CaO, more less TiO_2, more less MgO, FeO,
161E	Enclave-2	Gabbro	Mafic	Plagioclase, clinopyroxene, Fe-Ti oxide	Dominantly SiO_2, CaO, MgO, FeO rarely K_2O, Na_2O, TiO_2

3.2. LIBS data and PCA diagrams of the rocks

Measurement, detection and identification of the peaks of the each element in the LIBS spectra were carried out and spectra have been interpreted and evaluated by comparison these with NIST wavelength dataset which is available electronically. All major elements (Al, Si, Mg, Ca, Fe, O) presented in the major minerals of the rocks, some minors (K, Ti, Na, Mn, Cr) and some traces (Sr, Eu, Zr, La, Nb, Ta, Th, Sm, Sc, V) have been measured and defined on the spectra (Fig 5, 6 and, Table 3). It is noteworthy that some rare earth elements (La, Sm, Eu) and some light elements (Li, Na) could be measured with LIBS (Fig 5, 6 and, Table 3). Especially in enclaves, more elements could be measured and more significant peaks were obtained. While most elements were measured in all investigated rocks, some elements were detected only in host-1 and enclave-1 (Tm), and some were observed only in both enclaves (Sc). Zinc and Li are key elements for clarifying the crustal material addition of the composition of the rocks (Foley et al., 2013) and these elements may be measured by LIBS easily rather than the other conventional analytical techniques. Obtained LIBS data reveal that both enclaves and their hosts contain Li element (Fig 5, 6 and, Table 3).

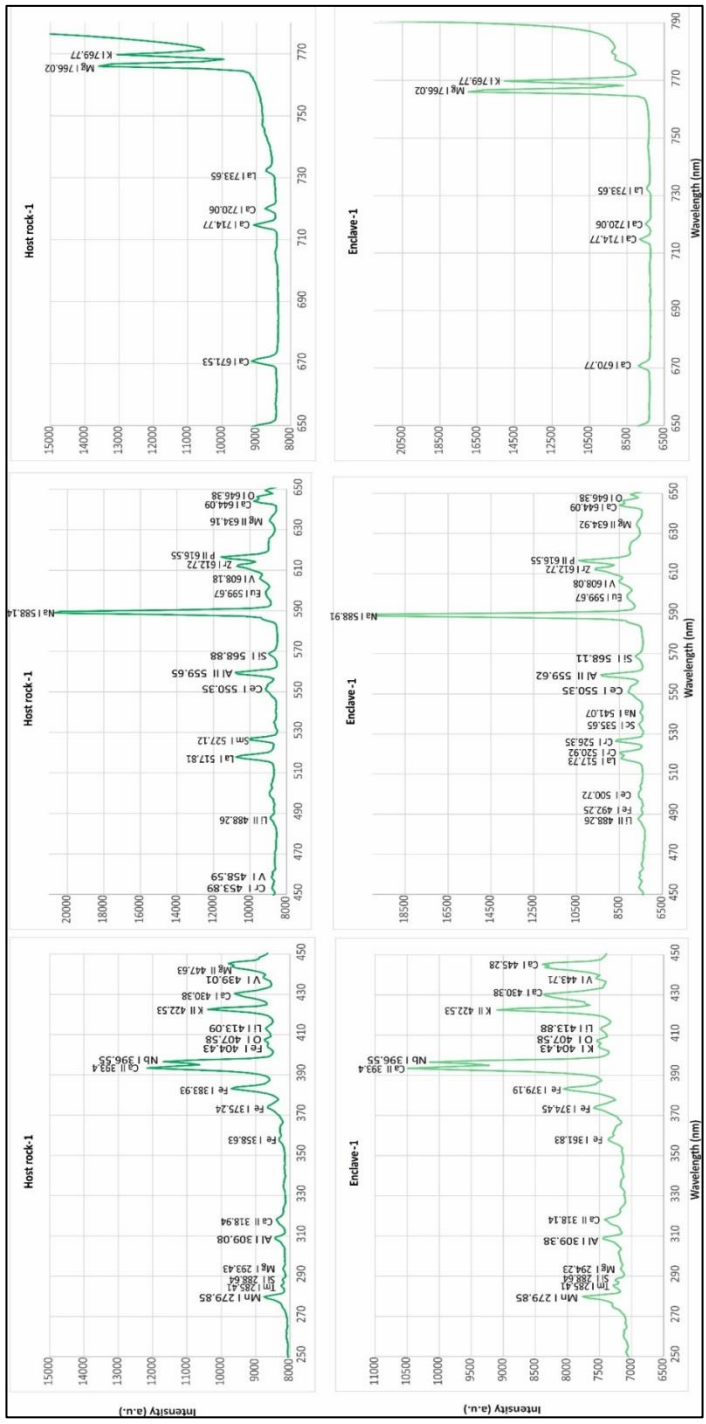

Fig. 5 Elements wavelength vs intensity plots of the Host rock-1 and Enclave-1

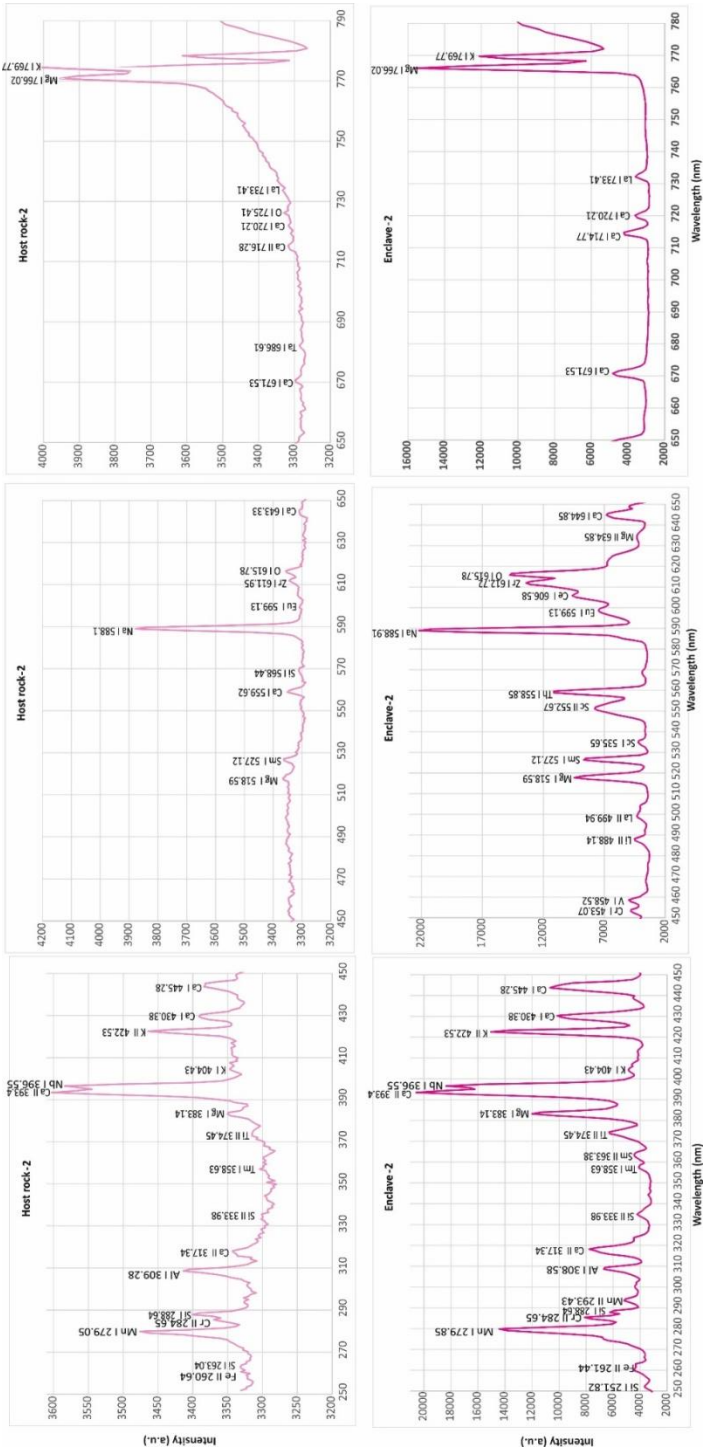

Fig. 6 Elements wavelength vs intensity plots of the Host rock-2 and Enclave-2

Table 3 LIBS data of the investigated rocks and their enclaves

Host rock-1			Enclave-1			Host rock-2			Enclave-2		
Observed Peak	Nist Peak	Element	Observed Peak	Nist Peak	Element	Observed Peak	Nist Peak	Element	Observed Peak	Nist Peak	Element
279.85	279.82	Mn-I	279.85	279.82	Mn-I	260.64	260.65	Fe-II	251.82	251.92	Si-I
285.45	285.41	Tm-I	285.45	285.41	Tm-I	263.04	263.12	Si-I	261.44	261.38	Fe -II
288.64	288.15	Si-I	288.64	288.15	Si-I	279.85	279.82	Mn-I	279.85	279.82	Mn-I
293.43	293.84	Mg-I	294.23	293.84	Mg-I	284.65	284.32	Cr-II	284.65	284.32	Cr-II
309.38	309.28	Al-I	309.38	309.28	Al-I	288.64	288.15	Si-I	287.84	287.95	Mn -II
318.94	318.28	Ca-II	318.14	318.28	Ca-II	309.28	309.28	Al-I	288.64	288.15	Si-I
358.63	358.58	Fe-I	361.83	361.87	Fe-I	317.34	317.93	Ca-II	293.40	293.30	Mn -II
375.24	375.82	Fe-I	374.45	374.55	Fe-I	333.98	333.98	Si-II	308.58	308.21	Al-I
383.93	383.42	Fe-I	379.19	379.50	Fe-I	358.63	358.58	Fe-I	318.14	318.28	Ca-II
393.40	393.36	Ca-II	393.40	393.36	Ca-II	374.45	374.55	Fe -I	323.71	323.62	Fe -I
396.55	396.60	Nb-I	396.55	396.60	Nb-I	383.14	383.23	Mg-I	335.63	335.52	Fe -I
404.43	404.41	K-I	404.22	404.41	K-I	393.40	393.36	Ca-II	358.63	358.58	Fe-I
407.58	407.58	O-I	407.58	407.58	O-I	396.55	396.60	Nb-I	363.38	363.43	Sm-II
413.09	413.26	Li-I	413.88	413.26	Li-I	422.53	422.67	K-II	374.45	374.55	Fe -I
422.53	422.56	K-II	422.53	422.56	K-II	430.38	430.25	Ca-I	383.14	383.23	Mg-I
430.38	430.25	Ca-I	429.59	429.41	Zr-I	445.28	445.47	Ca-I	393.40	393.36	Ca-II
439.01	439.53	V-I	430.38	430.25	Ca-I	488.26	488.14	Li-II	396.55	396.60	Nb-I
447.63	448.12	Mg-II	439.01	439.53	V-I	518.59	518.36	Mg-I	404.43	404.41	K-I
458.89	458.64	V-I	443.71	443.78	V-I	527.12	527.14	Sm-I	406.01	406.02	Ti -I
488.26	488.14	Li-II	445.28	445.47	Ca-I	559.62	558.19	Ca-I	422.53	422.56	K-II
517.81	517.71	La-I	488.26	488.14	Li-II	568.44	568.44	Si-I	430.38	430.25	Ca-I
527.12	527.14	Sm-I	492.15	492.05	Fe-I	588.14	588.90	Na-I	443.71	443.78	V-I
500.72	500.90	Ce-I	500.72	500.90	Ce-I	599.67	599.28	Eu-I	453.11	453.60	Cr-I
550.35	552.41	Sr-I	517.81	517.73	La -I	611.95	612.20	Zr-I	458.59	458.64	V-I
559.65	559.33	Al-II	520.92	520.84	Cr-I	615.78	615.81	O-I	488.26	488.37	Li-II
588.14	588.90	Na-I	526.35	526.41	Cr-I	643.33	643.90	Ca-I	499.94	499.46	La-II
599.67	599.28	Eu-I	535.65	535.60	Sc-I	671.53	671.76	Ca-I	518.59	518.36	Mg-I
608.18	608.14	V-I	550.35	552.41	Sr-I	686.10	686.10	Ta-I	527.12	527.14	Sm-I
612.72	612.74	Zr-I	559.62	559.33	Al-II	716.28	716.54	Ca-II	535.65	535.60	Sc-I
616.55	616.55	P-II	568.11	568.44	Si-I	720.21	720.21	Ca-I	551.12	551.20	Ce -II
634.16	634.67	Mg-II	588.91	588.90	Na-I	725.41	725.41	O-I	558.85	558.70	Th-I
646.38	645.59	O-I	608.08	608.14	V-I	733.41	733.41	La-I	568.11	568.45	Si -I
650.20	650.40	Na-I	612.72	612.74	Zr-I	766.02	765.99	Mg-I	588.91	588.90	Na-I
671.53	671.76	Ca-I	616.55	616.55	P-II	769.77	769.89	K-I	599.13	599.28	Eu-I
714.77	714.81	Ca-I	634.92	634.67	Mg-I				606.58	606.95	Ce -I
733.65	733.41	La-I	644.09	644.98	Ca-I				612.72	612.74	Zr-I
766.02	765.99	Mg-I	646.38	645.59	O-I				615.78	615.81	O-I
769.77	769.89	K-I	670.77	671.76	Ca-I				634.85	634.67	Mg-I
			714.77	714.81	Ca-I				644.85	644.98	Ca-I
			720.06	720.21	Ca-I				671.53	671.76	Ca-I
			724.59	725.41	O-I				714.77	714.81	Ca-I
			733.65	733.41	La-I				720.21	720.22	Ca-I
			766.02	765.99	Mg-I				733.65	733.41	La-I
			769.77	769.89	K-I				766.02	765.99	Mg-I
									769.77	769.89	K-I

The host rocks and enclaves were successfully differentiated from each other by using principal component analysis (PCA) technique shown in fig 7. The studied rocks have overlapped in PCA1 but have been discriminated in PCA2. The enclaves are located in close circles with their hosts, which indicates that they are related to their hosts and that they may be crystal clusters which crystallized and separated from the same magma at an early stage (G. Gençoğlu Korkmaz et al., 2021). Moreover, it is interesting that the enclaves, which exhibit similar petrographical and geochemical features, are located in quite different areas with the PCA and show that they are different types of enclaves. It supports the idea that rather than the presence of a large gabbroic mass underground, and that the phases crystallized in the early phase were transported by convection and included in the hosts (G. Gençoğlu Korkmaz et al., 2021).

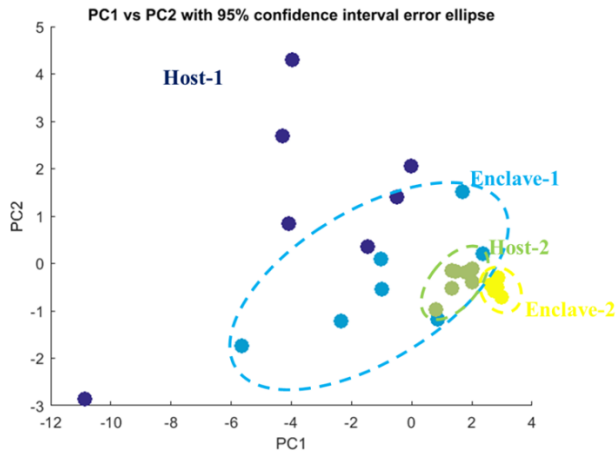

Fig.7 PCA diagram of the investigated rocks

3.3. Plasma characterization

To evaluate the laser-produced plasma based on the optical emission studies, the plasma should be optically thin and follows the local thermodynamic equilibrium (LTE) conditions (Umar et al., 2020). We used Ca I and II for all calculations and the Boltzmann plots. After the excitation temperature was calculated using the Boltzmann plot method(J. Aguilera & Aragón, 2007; J. A. Aguilera & Aragón, 2004), we evaluated the electron densities based on the NIST database and Corliss and Bozman (1966).

We have utilized the intensity ratio method for each sample to determine whether the plasma optical thickness was appropriate for the CF-LIB (Cremers & Radziemski, 2006; Unnikrishnan et al., 2012) .

$$\frac{I_1}{I_2} = \frac{A_1 g_1 \lambda_2}{A_2 g_2 \lambda_1} exp\left(-\frac{|E_1 - E_2|}{K_B T_e}\right) \quad (1)$$

I_1;I_2= Intensy (measured)

λ_1; λ_2= Wavelengths

A_1; A_2=Transition probability

g_1; g_2 = Statistical weights

E_1; E_2 = Upper level energies

K_B =Boltzmann constant,

T_e=Plasma temperature

We have calculated A and g values based on Corliss and Bozman (1966) by making interpolations according to upper and lower wavelength for each element having a spectral line (Supplementary files S1). To determine the intensity ratios, we have used the emission lines having the same or very close upper level energies to reduce the temperature dependence as in Umar et al. (2020). The measured intensity ratios and values evaluated from the NIST database 2018 and Corliss and Bozman (1966) are in accordance with eachother (<10%). Thus, produced-plasma for each sample satisfies the optically thin condition.

To execute LTE condition, the most critical factor is plasma temperature. The slope of Boltzmann plot yields the plasma temperature (Fig. 8). The Boltzmann plots of the investigated rocks are based on the selected calcium lines and exhibit a good linearity (R^2 values are close to 0). The plasma temperature of each samples has been detected from the slope of this line and ranges between 7724 and 5209.8 K (Table 4).

One of the most significant parameters is electron number density (Ne), is essential both for the plasma characterization as well as for the detection of chemical composition of any sample could be calculated by following Stark broadened line profile formula (Griem 1997; Cremers and Radziemski 2006):

$$\Delta\lambda_{1/2} = 2w\left(\frac{N_e}{10^{16}}\right) \quad (2)$$

where w is the Stark broadening parameter which is 0.00698 nm for Ca I line and $\lambda 1/2$ is the FWHM of the line due to Stark broadening. This requires that the electron number density in the plasma should exceed the certain critical value given by the McWhirter criterion (Cristoforetti, Aglio, & Legnaioli, 2009; Fujimoto & McWhirter, 1990). Therefore, calculated Ne values are correlated the values obtained from the following

McWhirter criterion formula;

$$N_e(cm^{-3}) \geq 1.6\, x\, 10^{12} T_e^{1/2} (\Delta E)^3 \quad (3)$$

where ΔE (eV) and T(K) are the energy differences between the upper and lower levels and plasma temperature obtained from the Boltzmann plots, respectively. The calculated electron number densities using the the Stark broadened line profile of Ca I at 393.4 nm are $1.038*10^{18}$, $1.07*10^{18}$, $7.879*10^{17}$, $2.1489*10^{19}$ which are much higher than estimated from formula 3 ($1.304*10^{15}$, $1.088*10^{15}$, $1.45*10^{15}$, $5.302*10^{12}$) (Table 4). According to all calculations, the plasma may be considered to be close to LTE and we can use the data measured by CF-LIBS method to calculate the chemical compositions of the rocks.

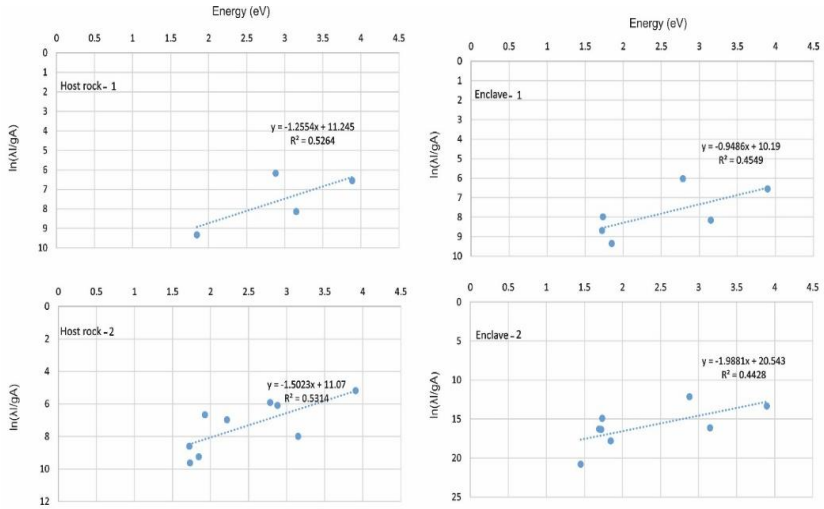

Fig.8 Boltzmann Plots of the investgated volcanic rocks and their enclaves

Table 4 The plasma characteristics of the investigated rocks and their enclaves

I(14H)	Element	Ionic T.	Wavelenght	Nist peak	A (*10^8/sec)	g	E (eV)	M (Slope)	T (K)	Ne
2537	Ca	II	318.94	318.28	3.09992378	0.48004573	3.88725152			
3133	Ca	II	393.4	393.36	0.905637931	0.20905172	3.15149975	-1.255380901	9243.766926	1.038*10^18
2776	Ca	I	430.38	430.25	5.759309021	1.62216891	2.88071007			
2682	Ca	I	671.53	671.76	0.23619381	0.15746254	1.84623174			
I(14E)	Element	Ionic T.	Wavelenght	Nist peak	A (*10^8/sec)	g	E (eV)	M (Slope)	T (K)	Ne
2538	Ca	II	318.14	318.28	3.09992378	0.48004573	3.89702647			
3189	Ca	II	393.4	393.36	0.905637931	0.20905172	3.15149975			
2849	Ca	I	445.28	445.47	6.849424084	2.00900524	2.78431549	-0.948582622	12233.46093	1.075*10^18
2724	Ca	I	670.77	671.76	0.23619381	0.15746254	1.84832357			
2806	Ca	I	714.77	714.81	0.949257788	0.72940414	1.73454398			
2711	Ca	I	720.06	720.21	0.455005551	0.35147483	1.72180096			
I(16H)	Element	Ionic T.	Wavelenght	Nist peak	A (*10^8/sec)	g	E (eV)	M (Slope)	T (K)	Ne
2526	Ca	II	317.34	317.93	14.09317073	2.21073171	3.9068507			
2714	Ca	II	393.4	393.36	0.905637931	0.20905172	3.15149975			
2545	Ca	I	430.38	430.25	5.759309021	1.62216891	2.88071007			
2538	Ca	I	445.28	445.47	6.849424084	2.00900524	2.78431549			
2521	Ca	I	559.62	558.19	2.35	1.102	2.2154319	-1.50231838	7724.360295	7.879*10^17
2490	Ca	I	643.33	643.9	3.148181818	0.00909462	1.92716024			
2465	Ca	I	671.53	671.76	0.23619381	0.15746254	1.84623174			
2473	Ca	II	716.28	716.54	0.13659675	0.46261392	1.73088736			
2489	Ca	I	720.06	720.2194	0.455005551	0.35147483	1.72180096			
I(16E)	Element	Ionic T.	Wavelenght	Nist peak	A (*10^8/sec)	g	E (eV)	M (Slope)	T (K)	Ne
2886	Ca	II	318.14	318.28	3.09992378	0.48004573	3.89702647			
4891	Ca	II	393.4	393.36	0.905637931	0.20905172	3.15149975			
4101	Ca	I	430.38	430.25	5.759309021	1.62216891	2.88071007			
3033	Ca	I	671.53	671.76	0.236071816	0.15738121	1.84623174			
2951	Ca	I	714.77	714.81	0.949257788	0.72940414	1.73454398	-0.222739121	52098.83384	2.1489*10^19
2812	Ca	I	720.06	720.2194	0.455005551	0.35147483	1.72180096			
2815	Ca	I	732.14	732.6146	0.468850436	0.36885044	1.69339197			
2877	Ca	II	854.09	854.2	0.045882097	0.04978759	1.45160346			

4. Conclusions

The identification/classification of the volcanic rocks and their enclaves outcropped the Karapınar-Karacadağ area (Konya-Turkey) was realized by utilizing CF–LIBS. Also, here we correlated these results with previous XRF data. According to LIBS data and previous XRF data, the major elements measured and defined by both methods were O, Si, Al, Ca, Mg, and Fe along with the minors of K, Ce, La, Sr, and Zr. Except for these elements, some rare earths (Sm, Eu, Tm) and light elements (Li, Na) which are paramount for the ore mineralogist and petrologists are measured by the LIBS. The chemical compositions of the rocks estimated using both techniques were in a harmony with each other.

For the application of CF-LIBS, the plasma temperature and electron density are obtained from the Boltzmann plot and Starkbroadened profile of Ca I-393.4 nm respectively as a function of incident laser energies. These plasma parameters are convenient for the CF-LIBS technique to evaluate the concentration of all the elements in the investigated rocks.

Based on all obtained results we could report that LIBS can be used for analytical analysis of the rocks without the need of huge sample preparations or complicated technical procedures. The implementation of the CF-LIBS method is useful for practical application in the rapid analysis of the composition of any rock and mineral. Both petrologically and economically critical elements such as rare earth elements and light elements could be

detected easily by the CF-LIBS. The rocks having petrographical properties and chemical compositions were very close to each other could be discriminate each other easily by using PCAs with the help of LIBS data. PCA diagrams of the investigated rocks reveal that both enclaves and host rocks are different from each other. However, it can be said that each enclave exhibits a composition close to its own host. In other words, it could be inferred that each enclave is related to its own host rock and is chemically similar to the composition of its host. That supports the idea that these enclaves are MSE enclaves consisting of early crystallized phases associated with the host rock, as mentioned in the previous studies (G. Gençoğlu Korkmaz et al., 2021).

5. References

Abedin, K. M., Haider, A., Rony, M., & Khan, Z. (2011). Identification of multiple rare earths and associated elements in raw monazite sands by laser-induced breakdown spectroscopy. *Optics & Laser Technology, 43*, 45-49. doi:10.1016/j.optlastec.2010.05.003

Aguilera, J., & Aragón, C. (2007). Multi-element Saha–Boltzmann and Boltzmann plots in laser-induced plasmas. *Spectrochimica Acta Part B: Atomic Spectroscopy, 62*(4), 378-385.

Aguilera, J. A., & Aragón, C. (2004). Characterization of a laser-induced plasma by spatially resolved spectroscopy of neutral atom and ion emissions.: Comparison of local and spatially integrated measurements. *Spectrochimica Acta Part B: Atomic Spectroscopy, 59*(12), 1861-1876.

Alberghina, M. F., Barraco, R., Brai, M., Schillaci, T., & Tranchina, L. (2011). Comparison of LIBS and μ-XRF measurements on bronze alloys for monitoring plasma effects. *Journal of Physics: Conference Series, 275*, 012017. doi:10.1088/1742-6596/275/1/012017

Barbarin, B., & Didier, J. (1991). *Enclaves and granite petrology*.

Barbarin, B., & Didier, J. (1992). Genesis and evolution of mafic microgranular enclaves through various types of interaction between coexisting felsic and mafic magmas. *Earth and Environmental Science Transactions of the Royal Society of Edinburgh, 83*(1-2), 145-153.

Best, M. G. (2003). *Igneous and metamorphic petrology* (2 ed.): John Wiley & Sons.

Bhatt, C., Jain, J., Goueguel, C., McIntyre, D., & Singh, J. (2018). Determination of Rare Earth Elements in Geological Samples Using Laser-Induced Breakdown Spectroscopy (LIBS). *Appl Spectrosc, 72*, 114-121. doi:10.1177/0003702817734854

Cantagrel, J.-M., Didier, J., & Gourgaud, A. (1984). Magma mixing: origin of intermediate rocks and "enclaves" from volcanism to plutonism. *Physics of the Earth and Planetary Interiors, 35*(1), 63-76. doi:https://doi.org/10.1016/0031-9201(84)90034-7

Corliss, C., & Bozman, W. (1966). Experimental transition probabilities for spectral lines of seventy elements; derived from the NBS Tables of spectral-line intensities.

Cousin, A., Sautter, V., Fabre, C., Maurice, S., & Wiens, R. C. (2012). Textural and modal analyses of picritic basalts with ChemCam Laser-Induced Breakdown Spectroscopy. *Journal of Geophysical Research: Planets, 117*(E10). doi:https://doi.org/10.1029/2012JE004132

Cremers, D. A., & Radziemski, L. J. (2006). Basics of the LIBS Plasma. *Handbook of Laser-Induced Breakdown Spectroscopy*, 23-52.

Cristoforetti, G., Aglio, M. D., & Legnaioli, S. (2009). Local thermodynamic equilibrium in laser-induced breakdown spectroscopy: Beyond the McWhirter criterion beyond the McWhirter criterion. *Spectrochim. Acta Part B, 65*, 86-95.

Dahlquist, J. (2002). *Mafic microgranular enclaves: Early segregation from metaluminous magma (Sierra de Chepes), Pampean Ranges, NW Argentina* (Vol. 15).

De Lucia, F. C., & Gottfried, J. L. (2011). Rapid analysis of energetic and geo-materials using LIBS. *Materials Today, 14*(6), 274-281. doi:https://doi.org/10.1016/S1369-7021(11)70142-0

Didier, J. (1991). The different types of enclaves in granites-Nomenclature. *Enclaves and granite petrology*.

Foley, S. F., Prelevic, D., Rehfeldt, T., & Jacob, D. E. (2013). Minor and trace elements in olivines as probes into early igneous and mantle melting processes. *Earth and Planetary Science Letters, 363*, 181-191. doi:https://doi.org/10.1016/j.epsl.2012.11.025

Fujimoto, T., & McWhirter, R. W. P. (1990). Validity criteria for local thermodynamic equilibrium in plasma spectroscopy. *Physical Review A, 42*(11), 6588-6601. doi:10.1103/PhysRevA.42.6588

Gençoğlu Korkmaz, G., Gündoğdu, Y., Kılıç, H. Ş., & Kurt, H. (2021, 10-12 April). *Determınatıon Of The Element Contents Of The Geologıcal Rock Samples Wıth The Help Of Cf-Lıbs.* Paper presented at the II.Internatıonal Hazar Scıentıfic Researchesconference, Khazar University, Baku, Azerbaijan.

Gençoğlu Korkmaz, G., Kurt, H., & Asan, K. (2021). Classification and Generation of the Enclaves in Karapınar-Karacadağ Volcanic Rocks (Central Anatolia). *Turkish Journal of Geosciences*, 30-46. doi:10.48053/turkgeo.1018063

Gill, R. (2010). Igneous Rocks and Processes: A Practical Guide. *The Geographical Journal, 176*(4), 375-376. doi:doi:10.1111/j.1475-4959.2010.00380_9.x

Gondal, M. A., Nasr, M. M., Ahmed, Z., & Yamani, Z. H. (2009). Determination of trace elements in volcanic rock samples collected from cenozoic lava eruption sites using LIBS. *Journal of Environmental Science and Health Part A, 44*(5), 528-535.

Gottfried, J. L., Harmon, R. S., De Lucia, F. C., & Miziolek, A. W. (2009). Multivariate analysis of laser-induced breakdown spectroscopy chemical signatures for geomaterial classification. *Spectrochimica Acta Part B: Atomic Spectroscopy, 64*(10), 1009-1019. doi:https://doi.org/10.1016/j.sab.2009.07.005

Hamad, T., Alaa, H., Salloom, H., & Ghazai, A. (2018). Calibration Free Laser Induced Breakdown Spectroscopy (CF-LIBS) as a tool for Quantitative Elemental Analysis of Iraqi Cement. doi:10.22401/SIC.I.08]

Hark, R., & Harmon, R. (2014). Geochemical Fingerprinting Using LIBS. *Laser-Induced Breakdown Spectroscopy Theory and Applications, 182*, 309-344. doi:10.1007/978-3-642-45085-3-12

Harmon, R., Remus, J., McMillan, N., McManus, C., Collins, L., Gottfried, J., . . . Miziolek, A. (2009). LIBS analysis of geomaterials: Geochemical fingerprinting for the rapid analysis and discrimination of minerals. *Applied Geochemistry, 24*, 1125-1141. doi:10.1016/j.apgeochem.2009.02.009

Harmon, R. S., Lawley, C. J. M., Watts, J., Harraden, C. L., Somers, A. M., & Hark, R. R. (2019). Laser-Induced Breakdown Spectroscopy—An Emerging Analytical Tool for Mineral Exploration. *Minerals, 9*(12), 718. Retrieved from https://www.mdpi.com/2075-163X/9/12/718

Harmon, R. S., Remus, J., McMillan, N. J., McManus, C., Collins, L., Gottfried, J. L., . . . Miziolek, A. W. (2009). LIBS analysis of geomaterials: Geochemical fingerprinting for the rapid analysis and discrimination of minerals. *Applied Geochemistry, 24*(6), 1125-1141. doi:https://doi.org/10.1016/j.apgeochem.2009.02.009

Harmon, R. S., Russo, R. E., & Hark, R. R. (2013). Applications of laser-induced breakdown spectroscopy for geochemical and environmental analysis: A comprehensive review. *Spectrochimica Acta Part B: Atomic Spectroscopy, 87*, 11-26.

Harmon, R. S., Throckmorton, C. S., Hark, R. R., Gottfried, J. L., Wörner, G., Harpp, K., & Collins, L. (2018). Discriminating volcanic centers with handheld laser-induced breakdown spectroscopy (LIBS). *Journal of Archaeological Science, 98*, 112-127. doi:https://doi.org/10.1016/j.jas.2018.07.009

Ilbeyli, N., & Pearce, J. (2005). *Petrogenesis of Igneous Enclaves in Plutonic Rocks of the Central Anatolian Crystalline Complex, Turkey* (Vol. 47).

Kadioglu, Y. K., & Gülec, N. (1996). Mafic Microgranular Enclaves and Interaction Between Felsic and Mafic Magmas in the Agacoren Intrusive Suite: Evidence from Petrographic Features and Mineral Chemistry. *International Geology Review, 38*(9), 854-867.

Kadıoğlu, Y. K., & Güleç, N. (1999). Types and genesis of the enclaves in Central Anatolian granitoids. *Geological Journal, 34*, 243-256. doi:10.1002/(SICI)1099-1034(199907/09)34:3<243::AID-GJ825>3.0.CO;2-#

Kalam, S. A., Rao, S. B. M., Jayananda, M., & Rao, S. V. (2020). Standoff femtosecond filament-induced breakdown spectroscopy for classification of geological materials. *Journal of Analytical Atomic Spectrometry, 35*(12), 3007-3020.

Kocak, K., Zedef, V., & Kansun, G. (2011). Magma mixing/mingling in the Eocene Horoz (Nigde) granitoids, Central southern Turkey: evidence from mafic microgranular enclaves. *Mineralogy and Petrology, 103*(1-4), 149-167. doi:10.1007/s00710-011-0165-7

Kumar, S. (2010). Mafic to hybrid microgranular enclaves in the Ladakh batholith, northwest Himalaya: Implications on calc-alkaline magma chamber processes. *Journal of the Geological Society of India, 76*(1), 5-25. doi:10.1007/s12594-010-0080-2

Kumar, S., Rino, V., & Pal, A. (2004). Field evidence of magma mixing from microgranular enclaves hosted in Palaeoproterozoic Malanjkhand granitoids, central India. *Gondwana Research, 7*(2), 539-548.

Kumar, S., & Singh, R. (2014). *Modelling of Magmatic and Allied Processes*.

Lasheras, R., Bello-Gálvez, C., & Anzano, J. (2010). Identification of polymers by libs using methods of correlation and normalized coordinates. *Polymer testing, 29*(8), 1057-1064.

Lawley, C. J. M., Somers, A. M., & Kjarsgaard, B. A. (2021). Rapid geochemical imaging of rocks and minerals with handheld laser induced breakdown spectroscopy (LIBS). *Journal of Geochemical Exploration, 222*, 106694. doi:https://doi.org/ 10.1016/j. gexplo. 2020.106694

Le Bas, M. J., Le Maitre, R. W., Streckeisen, A., & Zanettin, B. A. (1986). A Chemical Classification of Volcanic Rocks Based on the Total Alkali-Silica Diagram. *J. Petrol, 127*, 745.

Miziolek, A. W., Palleschi, V., & Schechter, I. (2006). *Laser induced breakdown spectroscopy*: Cambridge university press.

Muhammed Shameem, K. M., Dhanada, V. S., Harikrishnan, S., George, S. D., Kartha, V. B., Santhosh, C., & Unnikrishnan, V. K. (2020). Echelle LIBS-Raman system: A versatile tool for mineralogical and archaeological applications. *Talanta, 208*, 120482. doi:https://doi.org/ 10.1016/j.talanta.2019.120482

Musazzi, S., & Perini, U. (2014). Laser-induced breakdown spectroscopy. *Springer Series in Optical Sciences, 182*.

Noyes, J. H., A.F., F., & Wones, D. R. (1983). *A Tale of Two Plutons: Geochemical Evidence Bearing on the Origin and Differentiation of the Red Lake and Eagle Peak Plutons, Central Sierra Nevada, California* (Vol. 91).

Özdamar, Ş., Zou, H., Billor, Z., & Hames, W. (2020). Petrogenesis of mafic microgranular enclaves (MMEs) in the Oligocene-Miocene granitoid plutons from northwest Anatolia, Turkey. *Geochemistry*, 125713. doi:10.1016/j.chemer.2020.125713

Panya panya, S. N., Galmed, A. H., Maaza, M., Mothudi, B. M., Harith, M. A., & Kennedy, J. (2018). Laser-Induced Breakdown Spectroscopy (LIBS) on Geological Samples: Compositional Differentiation. *MRS Advances, 3*(34-35), 1969-1983. doi:10.1557/adv.2018.401

Remus, J., Gottfried, J., Harmon, R., Draucker, A., Baron, D., & Yohe, R. (2010). Archaeological Applications of Laser-induced Breakdown Spectroscopy: An Example from the Coso Volcanic Field, California, Using Advanced Statistical Signal Processing Analysis. *Applied Optics - APPL OPT, 49*. doi:10.1364/AO.49.00C120

Rollinson, H. R. (1993). Using geochemical data: evaluation. *Presentation, interpretation. Singapore. Ongman*.

Roux, C. P. M., Rakovský, J., Musset, O., Monna, F., Buoncristiani, J. F., Pellenard, P., & Thomazo, C. (2015). In situ Laser Induced Breakdown Spectroscopy as a tool to discriminate volcanic rocks and magmatic series, Iceland. *Spectrochimica Acta Part B: Atomic Spectroscopy, 103-104*, 63-69. doi:https://doi.org/ 10.1016/j .sab.2014.11.013

Tognoni, E., Cristoforetti, G., Legnaioli, S., & Palleschi, V. (2009). Calibration-Free Laser-Induced Breakdown Spectroscopy: State of the art. *Spectrochimica Acta Part B: Atomic Spectroscopy*, 1-14. doi:10.1016/j.sab.2009.11.006

Umar, Z. A., Liaqat, U., Ahmed, R., & Baig, M. A. (2020). Classification of nephrite using calibration-free laser induced breakdown spectroscopy (CF–LIBS) with comparison to laser ablation–time-of-flight–mass spectrometry (LA–TOF–MS). *Analytical Letters, 53*(2), 203-216.

Unnikrishnan, V., Mridul, K., Nayak, R., Alti, K., Kartha, V., Santhosh, C., . . . Suri, B. (2012). Calibration-free laser-induced breakdown spectroscopy for quantitative elemental analysis of materials. *Pramana, 79*(2), 299-310.

Winter, J. D. (2001). *An introduction to igneous and metamorphic petrology*: Prentice Hall, Upper Saddle River.

Wold, S., Esbensen, K., & Geladi, P. (1987). Principal component analysis. *Chemometrics and intelligent laboratory systems, 2*(1-3), 37-52.

Yueh, F.-Y., Zheng, H., Singh, J. P., & Burgess, S. (2009). Preliminary evaluation of laser-induced breakdown spectroscopy for tissue classification. *Spectrochimica Acta Part B: Atomic Spectroscopy, 64*(10), 1059-1067.

Zhang, G., Peng, R., Qiu, H., Wen, H., Feng, Y., Chen, B., . . . Liu, T. (2020). Origin of Northeast Fujian Basalts and Limitations on the Heterogeneity of Mantle Sources for Cenozoic Alkaline Magmatism across SE China: Evidence from Zircon U-Pb Dating, Petrological, Whole-Rock Geochemical, and Isotopic Studies. *Minerals, 10*(9), 770.